Supplementary Information

In vivo **biogenesis of a** ***de novo*** **designed iron-sulfur protein**

Bhanu P. Jagilinki, Stefan Ilic, Cristian Trncik, Alexei M. Tyryshkin, Douglas H. Pike, Wolfgang Lubitz, Eckhard Bill, Oliver Einsle, James A. Birrell, Barak Akabayov, Dror Noy, Vikas Nanda

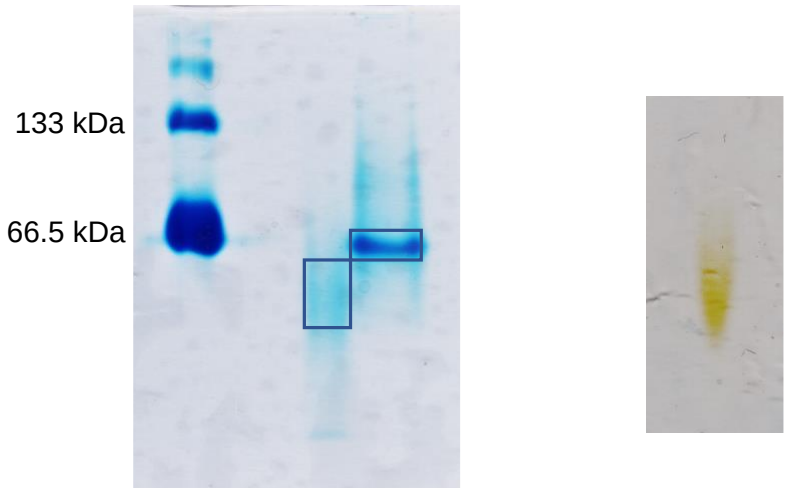

Figure S1. (A) Native anaerobic gel of biologically assembled holo-CCIS in low salt and high salt, stained with Coomassie Brilliant Blue. Lane 1: BSA; Lane 3: holo-CCIS in low salt and Lane 4: holo-CCIS in high salt **(B)** Native anaerobic gel without stain showing the yellow color of the holo-CCIS in low salt..

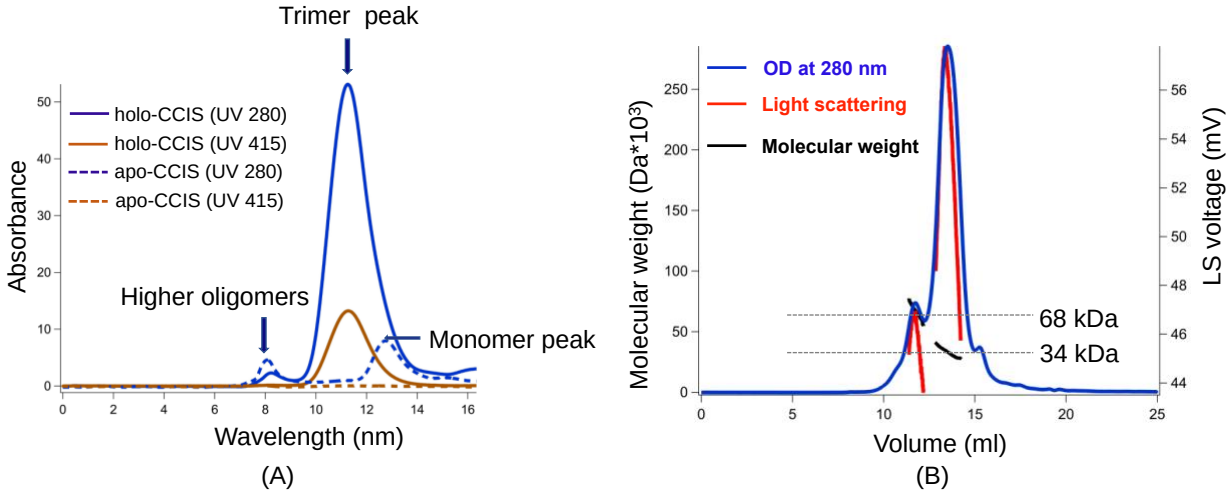

Figure S2. **(A)** Size-exclusion chromatograms (SEC) of holo-CCIS and apo-CCIS. The chromatogram of biologically assembled holo-CCIS performed anaerobically, on GE Superdex 75 10/300 GL column is shown in thick lines. The chromatogram of apo-CCIS performed aerobically, is shown in broken lines. The blue line corresponds to absorbance at 280 nm while the brown line corresponds to 415 nm. This chromatogram confirms the trimeric nature of the biologically assembled holo-CCIS and the absorbance at 415 nm suggests the FeS cluster is intact throughout the run. **(B)** SEC-LS of holo-CCIS. The chromatogram as analyzed by UV 280 nm wavelength (in dark blue) and LS voltage (red). The molecular weight trace is in black and the scale is on the left hand side. The major peak has a molecular weight of ≈34 kDa, which is three times the mass of monomeric CCIS.

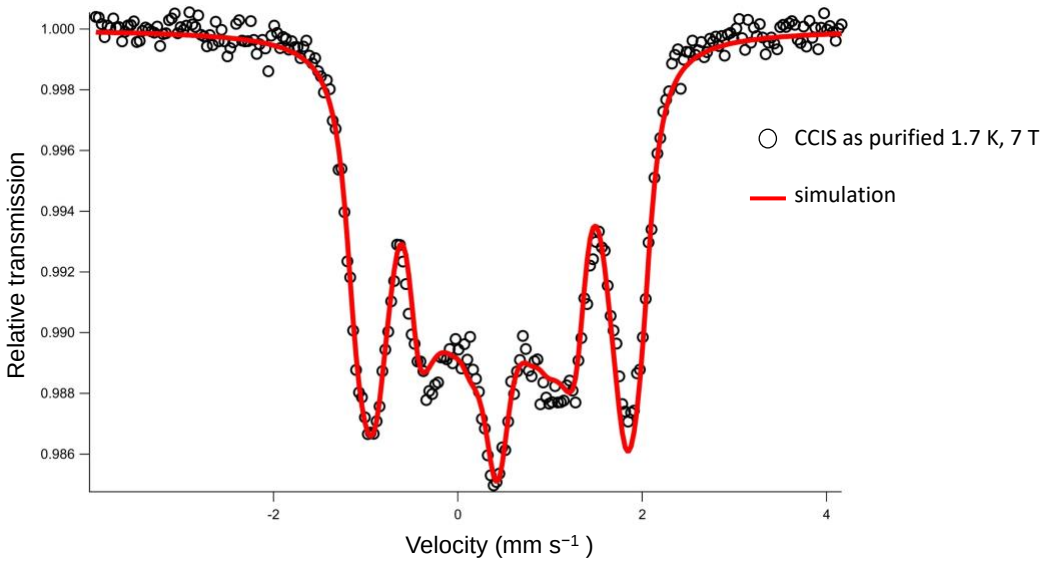

Figure S3 (A): Mössbauer spectrum of 1 mM CCIS at a temperature of 1.7 K and with a 7 T magnetic field applied perpendicular to the γ-beam. Empty circles represent the experimental data and the solid red line is a single component simulation (assuming all four Fe are identical) using an isomer shift of 0.44 mm/s, a quadrupole splitting of -1.04 mm/s, an asymmetry parameter (η) of 0.9, and a line width of 0.26 mm/s. Fitting was performed using in-house routines. (1)

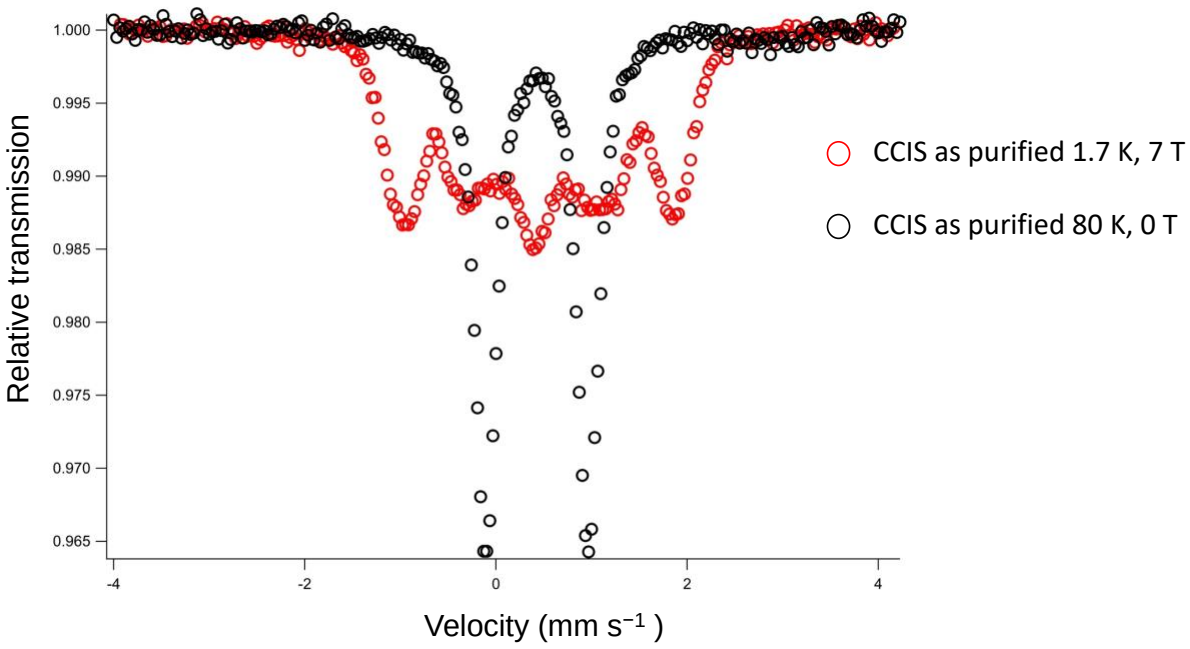

Figure S3 (B): Mössbauer spectra of 1 mM CCIS at a temperature of 80 K and with no applied magnetic field (black circles) and at a temperature of 1.7 K and with a 7 T magnetic field applied perpendicular to the γ-beam (red circles). Both Mössbauer spectra of CCIS are consistent with other observations of S = 0 [4Fe-4S] clusters in a valence delocalized $Fe^{2.5+}$ state (2). The difference in the appearance of the spectrum at 1.7 K and 7 T in comparison with that measured at 80 K and 0 T is due to weak magnetic interactions of the ^{57}Fe nuclei with the applied field.

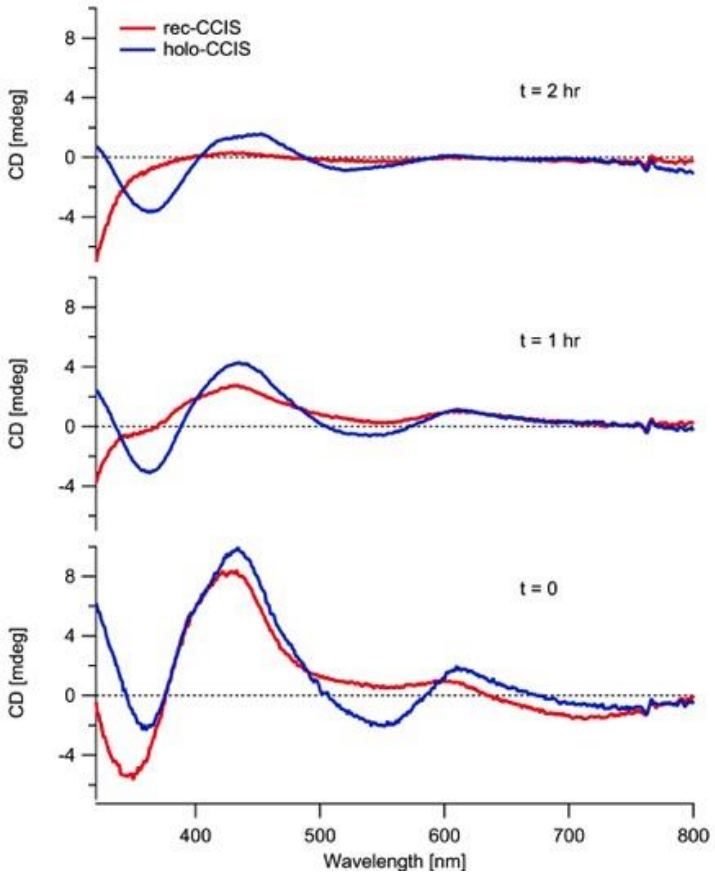

Figure S4. CD in visible region in presence of oxygen. The blue line corresponds to holo-CCIS, whereas the red is rec-CCIS. The bottom graph is at time zero, whereas the top graphs are recorded after one and 2 hours respectively. These spectra confirm that the rec-CCIS is more oxygen sensitive than the holo-CCIS.

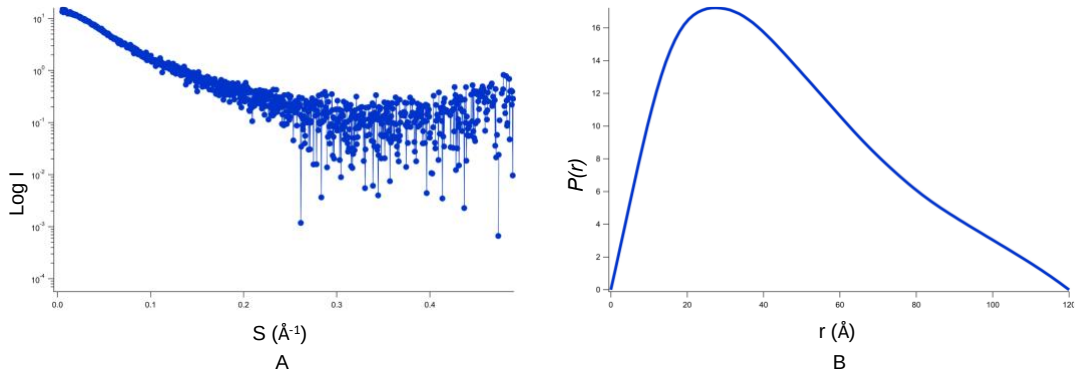

Figure S5. SAXS of the holo-CCIS. **(A)** Experimental SAXS scattering profile. **(B)** The distance distribution function P(r) obtained from GNOM, showing the Dmax as 120 Å. See supplementary methods for additional details on data collection and fitting.

SUPPLEMENTARY METHODS

Cloning and Mutagenesis. The nucleotide sequence coding CCIS was commercially procured and was cloned into Kanamycin based pET-28a (+) vector between BamHI and XhoI restriction sites. The N-terminal His tag was replaced with N-terminal strep tag, followed by a SUMO sequence with ULP protease and TEV protease cleavage sites. Site directed mutagenesis was performed to generate four different cysteine single mutants (C13, C17, C61 and C65) and two cysteine double mutants (C13 & C17) and (C61 & C65). In all these mutants, cysteine has been mutated to serine. Primers used for generating cysteine to serine mutants are as follows:

C13S single mutant forward primer:

5’ GCGTGGGAACGTTCTTGGCGTCAG

C17S single mutant forward primer:

5’ GGCGTCAGTCTCAGCAGCTG

C61S single mutant forward primer:

5’ GCACGCGCATCCGCTCAGCGTTGC

C65S single mutant forward primer:

5’ GCTCAGCGTTCCCAACGTCTG

C13S & C17S double mutant forward primer:

5’ GCGTGGGAACGTTCTTGGCGTCAGTCTCAGCAGCTGTCC

C61S & C65S double mutant forward primer:

5’ GACGCACGCGCATCCGCTCAGCGTTCCCAACGTCTGTC

For generating h1 truncated version of CCIS, a stop codon was incorporated into the Open reading frame (ORF) of CCIS plasmid just after the helix one. The primer sequence used to generate the h1 is given below:

5’ CTGTCCGAAAAATAGACCTCCAACCCG

A gradient PCR (Labcycler, SensoQuest) was performed between 55°C and 65°C using Phusion High-Fidelity DNA Polymerase (Finnzymes) with an elongation time of 3 minutes for 17 cycles. After confirming the SDM amplification on a 1% agarose gel, the sample was subjected to DpnI digestion. For DpnI digestion 7.5 µl of PCR amplified product, 2 ul of 10X Fast Digest Buffer (Thermo Fisher) and 0.5 µl of Fast Digest DpnI (Thermo Fisher) was added and total reaction volume was made up to 20 µl with distilled water and incubated at 37°C for 30 minutes. The DpnI digested sample was then transformed into DH5α competent cells. This method was followed individually for all the mutants generated. Following transformation, individual colony from each plate was grown into 10 ml of LB media at 37°C, 200 rpm. Following overnight growth, plasmid was isolated from each individual mutant.

Electron Paramagnetic Resonance (EPR). EPR samples were prepared by reducing holo-CCIS with sodium dithionite. Sodium dithionite (Sigma-Aldrich) was freshly prepared in 1 M Glycine pH 10.4 buffer. Holo-CCIS (final concentration 200 μM protein or 66 μM trimeric complex) and sodium dithionite (final concentration 20 mM) were combined (final pH 8.0) and 200 µl transferred into air-tight EPR quartz tubes and frozen in liquid nitrogen. All the EPR samples had 15% (v/v) glycerol as cryoprotectant.

The continuous-wave (CW) X-band EPR (ELEXSYS E580, Bruker) experiments were performed at a temperature of 10 K using a helium-flow cryostat (ESR900, Oxford Instruments) equipped with a temperature controller (ITC4, Oxford Instruments). Spin quantification of the reduced $[4Fe\text{-}4S]^{+}$ cluster concentration in the sample was performed by comparing the double integral of the measured EPR signal from $[4Fe\text{-}4S]^{+}$ with a reference signal from a known number of spins of a $CuSO_4.5(H_2O)$ crystal.

Mössbauer Spectroscopy. For Mössbauer spectroscopy, the bacterial cells were grown and induced in M9 media, supplemented with 10 mg/l of $^{57}FeSO_4$ as the only iron source. Mössbauer samples were prepared by concentrating ^{57}Fe-labelled CCIS to 1 mM, transferring the sample to 1 mL sample holders and freezing in liquid nitrogen. Mössbauer spectra were recorded on a conventional spectrometer with alternating constant acceleration cooled with an Oxford Instruments Variox cryostat, using a ^{57}Co/Rh (1.8 GBq) γ-source. Samples were measured at 80 K and with no applied magnetic field or 1.7 K with a 7 T magnetic field applied perpendicular to the γ-beam. Isomer shifts are relative to iron metal at 300 K. Spectra were simulated and fitted using Lorentzian quadrupole doublets using in-house software.

Size-Exclusion Chromatography, Static Light Scattering. To analyze the aggregation state of the biologically assembled holo-CCIS, Size-exclusion chromatography was performed anaerobically by using Superdex-75 10/300 GL (GE Life Sciences), connected to a Fast Protein Liquid Chromatography (FPLC) system (ÄKTA pure, GE Life Sciences). To maintain anaerobicity of the FPLC system, the

FPLC buffer (buffer B) was continuously purged with nitrogen throughout the run. After three column washes, 200 µl of 1.5 mg/ml of holo-CCIS was injected on to the column at 0.5 ml/minute flow rate. The absorbance at 280 nm and 415 nm were monitored. Similarly, for apo-protein, 200 µl of 0.25 mg/ml apo-CCIS was injected onto the FPLC column and the chromatogram was performed aerobically.

To calculate the accurate molecular mass and determine the oligomeric state of biologically assembled holo-CCIS, Static Light Scattering (SLS) was performed (3). To this end, the protein was injected anaerobically on to a Superdex-200 column, coupled to Light Scattering (LS), UV and Refraction Index detectors. Three different concentrations (1, 5 and 7.5 mg/ml) of protein were injected at 0.1 ml/minute. The sample was maintained anaerobic throughout by continuous nitrogen purging of the buffer. The light-scattering detector was turned on only when there was a peak detected by UV at 280 nm, and was turned off when there was no protein peak. The data obtained from SLS was analyzed as described by Slotboom et al (4). Before injecting, holo-CCIS, the system was calibrated by running BSA at 1, 5 and 7.5 mg/ml concentrations.

UV-visible and CD Spectroscopy. Optical absorption spectra were recorded with a Jasco V-7200 Spectrophotometer, (Jasco, Japan). A 1 cm^2 quartz air-tight cuvette was used for air-sensitive samples such as biologically assembled holo-CCIS. Alternatively, samples were measured in a cuvette using a Nano-drop (Thermo Scientific) inside an

anaerobic chamber. Typically, 1 mg/ml solutions of holo-CCIS were used for absorption spectroscopy.

Circular Dichroism Spectroscopy (Chirascan-plus, Applied Photophysics) was performed in the visible region to study the effect of circularly polarized light on the FeS cluster (5-7). 2 ml of 200 µM holo-CCIS in a 1 cm pathlength cuvette was used to measure the CD spectrum in the visible region. For the thermal stability assay of the FeS cluster, CD spectra from 20°C to 80 °C were recorded. Each subsequent spectrum has an increment of 2 °C and incubation time of 10 minutes.

CD spectroscopy was also used to study the secondary structure of CCIS in the far UV region and oxygen sensitivity in the visible region. For secondary structure analysis, 200 µl of 12 µM of protein in buffer B (5 mM Tris-HCl pH 8.0, 20 mM NaCl) in a 1 mm quartz cuvette, was taken and CD spectra were recorded between 250-195 nm. CD spectra were recorded both for apo and holo-CCIS. Thermal denaturation was performed for holo-CCIS by recording the initial spectrum at 10 °C and each successive spectrum was recorded with an increment of 2 °C and incubation time of 8 minutes. For the oxygen sensitivity assay, the CD spectrum in the visible region was recorded for 750 minutes, obtaining spectra for every 30 minutes. This experiment was performed both for holo-CCIS and the rec-CCIS.

Thermal Denaturation by CD. Thermal denaturation was performed using Circular Dichroism spectroscopy to characterize the thermal stability of the [4Fe-4S] cluster

present within the holo-CCIS. 2 ml of 200 µM of protein in buffer B was taken in a 1 cm quartz cuvette, and CD spectra was recorded in visible region between 300-800 nm. Multiple spectra were recorded in the temperature range of 10 to 80 °C. Each successive spectrum was recorded after an increment of 2 °C with an incubation time of 10 minutes. The changes in the ellipticity corresponding to 400 nm were taken and converted to percentage inactivation, which is plotted against temperature. Although the melting curve follows a single transition, the pre-transition phase is non-linear. Considering this, a non-linear fit was performed using three temperature independent constants a, b and c, by slightly modifying the equation described by Yadav *et al* (8). The new equation is given as:

$$y(T) = \frac{(a_N + b_N(T) + c_N(T)^2) + (a_D + b_D(T) + c_D(T)^2)\exp[-\Delta H^{Van}/R(1/T-1/T_m)]}{1 + \exp[-\Delta H^{Van}/R(1/T-1/T_m)]}$$ --- Equation 1

Where, a, b and c are temperature independent constants, N and D are native and denatured states, ΔH^{Van} is change in enthalpy, R = 1.9872×10^{-3} kcal K^{-1} mol^{-1} and T is temperature in Kelvin.

Small-Angle X-ray Scattering (SAXS). SAXS data of holo-CCIS was collected at the BioSAXS beamline BM29 (ESRF, Grenoble, France), using the Pilatus 1M detector. The scattering intensity was recorded at an interval of $0.0035 < q < 0.49$ $Å^{-1}$. The measurements were performed at 20 °C. The SAXS data was collected at protein concentrations of 1.25, 1.50, 1.75, and 2.00 mg/ml. The scattering of the buffer was subtracted from the scattering of all the samples.

The SAXS data represent the correlation between the scattering intensity (I) and the magnitude of the scattering vector (q), given by the following equation:

$$\mathbf{q} = \frac{4\pi \sin\theta}{\lambda}$$ --- Equation 2

where, 2θ represents the scattering angle, and λ is the wavelength.

Radius of gyration (R_g) was derived from Guinier region using PRIMUS (9). In this region the following Guinier approximation is applicable:

$$I(\mathbf{q}) = I(0)\mathrm{e}^{-R_g^2 q^2/3}$$ --- Equation 3

R_g and the distance distribution function *P(r)* were calculated using *in house* scripts as reported in (10). Briefly, this script performs an automatic search for the best fitting parameters in GNOM (11). The results were refined manually and are presented in **Table S1**. Molecular envelopes were constructed using DAMMIN and averaged using DAMAVER (12, 13) to obtain the final model.

Elemental analysis by ICP-AES. To measure the sulfur and iron content in holo-CCIS, Inductively coupled plasma atomic emission spectroscopy (ICP-OES 5110, Agilent) was performed. 100 µL of 1 mg/ml of holo-CCIS was digested overnight by incubating in 50 % HNO_3 at 90 °C. Following overnight digestion, the sample was diluted in double distilled water to get suitable HNO_3 concentration of about 2-2.5 %. Then the sample was centrifuged for 5 min at 4 °C at 6000 rpm. Similarly, blank sample was treated using buffer instead of the sample. The spectra were then acquired using the following emission wavelengths; 181.972 nm for sulfur and 238.204 nm for iron. Standard solutions were prepared in the range of 0.5 -100 ppm for sulfur and 0.1- 5.0 ppm for Fe.

The high-correlation coefficient values ($R^2 > 0.9997$) indicated good linearity for both sulfur and iron within the relatively wide concentration ranges. Reliable values less than 2% for relative standard deviation (RSD) were obtained for both sulfur and iron elements. The ratio between sulfur and iron atoms in the protein sample was then calculated and are presented in **Table S2**.

Protein concentration (mg/mL)	**Method**	**R_g (Å)**	**D_{max} (Å)**
1.25	Guinier	39.5 ± 1.87	
	P(r)	36.32	120
1.50	Guinier	41.4 ± 2.04	
	P(r)	36.53	118
1.75	Guinier	37.3 ± 1.27	
	P(r)	37.9	125
2.00	Guinier	43.5 ± 1.74	
	P(r)	37.62	130

Table S1: The table represents the protein concentrations on the left column and the measured paraments on the right columns from the SAXS data. R_g is radius of gyration and D_{max} maximum diameter of the particle.

Element	Blank (ppm)	holo-CCIS (ppm)	Corrected (ppm)	Content (µg)	Content (µmole)	S/Fe ratio
Fe	0.007648878	0.632272367	0.624623489	2.31110691	0.041380607	4.41
S	0.091625795	1.673298101	1.581672306	5.85218753	0.182510137	

Table S2. ICP-AES elemental analysis of iron and sulfur for holo-CCIS. Sample size is 100 µl of 1 mg/ml protein.

SUPPLEMENTAL REFERENCES

1. H. Beinert, R. H. Holm, E. Munck, Iron-sulfur clusters: nature's modular, multipurpose structures. *Science* **277**, 653-659 (1997).
2. C. L. Thompson *et al.*, Mossbauer effect in the eight-iron ferredoxin from Clostridium pasterurianum. Evidence for the state of the iron atoms. *The Biochemical journal* **139**, 97-103 (1974).
3. R. M. Murphy, Static and dynamic light scattering of biological macromolecules: what can we learn? *Current opinion in biotechnology* **8**, 25-30 (1997).
4. D. J. Slotboom, R. H. Duurkens, K. Olieman, G. B. Erkens, Static light scattering to characterize membrane proteins in detergent solution. *Methods* **46**, 73-82 (2008).
5. P. J. Stephens *et al.*, Circular dichroism and magnetic circular dichroism of iron-sulfur proteins. *Biochemistry* **17**, 4770-4778 (1978).
6. R. W. Woody, Circular dichroism. *Methods in enzymology* **246**, 34-71 (1995).
7. S. Ollagnier de Choudens, F. Barras, Genetic, Biochemical, and Biophysical Methods for Studying FeS Proteins and Their Assembly. *Methods in enzymology* **595**, 1-32 (2017).
8. S. Yadav, F. Ahmad, A new method for the determination of stability parameters of proteins from their heat-induced denaturation curves. *Analytical biochemistry* **283**, 207-213 (2000).
9. P. V. Konarev, V. V. Volkov, A. V. Sokolova, M. H. J. Koch, D. I. Svergun, PRIMUS: a Windows PC-based system for small-angle scattering data analysis. *Journal of Applied Crystallography* **36**, 1277-1282 (2003).
10. B. Akabayov *et al.*, Conformational dynamics of bacteriophage T7 DNA polymerase and its processivity factor, Escherichia coli thioredoxin. *Proceedings of the National Academy of Sciences of the United States of America* **107**, 15033-15038 (2010).
11. D. Svergun, A direct indirect method of small-angle scattering data treatment. *Journal of Applied Crystallography* **26**, 258-267 (1993).
12. D. I. Svergun, Restoring low resolution structure of biological macromolecules from solution scattering using simulated annealing. *Biophysical journal* **76**, 2879-2886 (1999).
13. V. V. Volkov, D. I. Svergun, Uniqueness of ab initio shape determination in small-angle scattering. *Journal of Applied Crystallography* **36**, 860-864 (2003).